Surface smoothness and conductivity control of vapor-phase polymerized poly(3,4-ethylenedioxythiophene) thin coating for flexible optoelectronic applications

Thuy Le Truong [a], Dong-Ouk Kim [a], Youngkwan Lee [b], Tae-Woo Lee [c], Jong Jin Park [c], Lyongsun Pu [c], Jae-Do Nam [a],*

[a] Department of Polymer Science and Engineering, SKKU Advanced Institute of Nanotechnology (SAINT), South Korea
[b] Department of Chemical Engineering, Sungkyunkwan University, 300 Chunchun-dong, Jangan-gu, Suwon, 440-746, South Korea
[c] Samsung Advanced Institute of Technology, Mt. 14-1, Nongseo-dong, Giheung-gu, Yongin-si, Gyeonggi-do 446-712, South Korea

Abstract

The surface morphology of poly(3,4-ethylenedioxythiophene) (PEDOT) was investigated in the vapor-phase polymerization of the thiophene monomer on a flexible polyethyleneterphthalate (PET) substrate film. The PET surface was modified with ethylene diamine maintaining the surface roughness within 2 nm to create amine and amide groups for the enhanced hydrophilic interaction with Fe(III)-tosylate (Fe(OTs)$_3$) and for the desirable hydrogen bonding with thiophene monomer as well as PEDOT. Polymerization rate was reduced by incorporating pyridine as a reaction retardant to control the surface roughness and conductivity of PEDOT thin films. The optimal conditions of pyridine and glycerol were found at a pyridine/Fe(OTs)$_3$ molar ratio of 0.5 and a glycerol concentration of 4–5 wt.%, respectively, providing the conductivity up to 500 S/cm and the surface roughness <2 nm.
© 2007 Elsevier B.V. All rights reserved.

1. Introduction

There have been many studies on poly(3,4-ethylenedioxythiophene) (PEDOT) over recent years on account of its many advantageous properties such as high conductivity, transparency and stability [1–3]. This makes PEDOT very attractive for applications including electrochromic windows [4], organic electrodes for photovoltaics [5,6] and hole transport layers of organic/polymer light emitting device [7–11]. In most of those optoelectronic applications as buffer or electrode layers, the interface with the PEDOT coating layer plays an important role in determining the operating characteristics, quantum efficiency and stability [12,13]. In general, the surface roughness of the PEDOT thin films is required not to exceed several nanometers (<10 nm), and a uniform composition is usually required.

Therefore, the main issues in most electronic device applications are not only the electrical conductivity but also the film surface morphology such as film thickness, surface roughness, uniformity, etc.

Oxidized PEDOT can be produced in several forms using different polymerization techniques. Solution processing is most commonly be used in synthesizing PEDOT in the form of spin-coating, solvent-casting, or ink-jet printing. However, the PEDOT system is relatively insoluble in most solvents, which makes it necessary to derivatize it with soluble side chains or dope the polymer with stabilizing polyelectrolytes [14]. One of the most widely used systems is an aqueous dispersion of poly(3,4-ethylenedioxythiophene)-poly(styrenesulfonate) (PEDOT–PSS), Baytron P, which is a stable polymer system with a high transparency up to 80% [15,16]. However, the PEDOT–PSS film exhibits a relatively low electrical conductivity, ~10 S/cm [15,16], which does not meet the high conductivity requirements in most applications. In addition, according to scanning-tunneling

---

* Corresponding author.
  E-mail address: jdnam@skku.edu (J.-D. Nam).

microscope and neutron reflectivity measurements, a PSS rich layer has been found at the top of the spin-coated PEDOT–PSS films [17–19]. An excessive amount of PSS is needed to stabilize the dispersion, and thus the final PEDOT–PSS films may contain substantial amounts of PSS that segregates from the PEDOT–PSS complex. Since PSS is an electrical insulator, the excessive PSS could limit the film conductivity [17]. Furthermore, PSS could degrade the performance of organic light emitting devices [20] because an acidic PEDOT–PSS solution can etch indium tin oxide (ITO) during the polymer spin-coating process, and the hydrolysis of the deposited PEDOT–PSS by moisture absorption can also etch ITO to cause indium incorporation into the polymer.

On the other hand, PEDOT can be deposited directly on the substrate surface by in-situ polymerization. This can be achieved by electrochemical polymerization, which has been reported to enhance the conductivity but results in a poor transparency [21]. However, electrochemical polymerization needs to be carried out on conducting substrates, which limits the practical applications of this method. In this sense, oxidative chemical polymerization is more versatile and less restricted by the substrate because chemical oxidation can be performed simply by coating the surface with a mixture containing the monomer and oxidant. Such mixtures have a limited pot-lifetime but more degrees of freedom in the process design and application can be achieved using separate pots containing monomer and oxidant.

One way to achieve this is to apply the oxidant using a solvent coating process and exposing the coated surface to a monomer vapor, which is often referred as vapor phase polymerization (VPP) [3,22,23]. PEDOT films produced by VPP have been reported to have conductivities of approximately 70 S/cm and light transmittance up to 95% below a 40 nm thickness using $FeCl_3$ as the oxidizing agent [22]. Recently, a PEDOT film with a high conductivity, exceeding 1000 S/cm was reported using a base-inhibited VPP [3]. However, it should be pointed out that the surface conductivity of thin films be measured for a very smooth surface, say, within a few nanometers of roughness to meet the device-assembly requirements and accurate measurements of conductivity. It should also be mentioned that the optimal treatment conditions of the base in the PEDOT VPP coating has not been identified in terms of the electrical conductivity and surface morphology.

Various additives can be used to improve the conductivity of PEDOT and its charge transport properties. For example, the addition of dopants such as glycerol and sorbitol modifies the PEDOT morphology and increases the conductivity [24–26]. It is believed that the screening effect of polar solvents such as dimethyl sulfoxide, N,N-dimethylformamide, or tetrahydrofuran plays an important role in transporting charges between the PSS and PEDOT polymer main chains [27]. It has also been reported that the PF_6^- doping chemically modifies PEDOT during the anodic oxidation of EDOT to give an improved conductivity [28]. In particular, weak bases such as imidazole [29,30], and pyridine [3] have been reported to reduce the polymerization reaction kinetics enhancing the conductivity and transparency of the PEDOT coating. In the device applications of PEDOT thin films, however, these additive techniques need to be optimized to provide smooth surface morphology as well as balanced properties of electrical and optical characteristics.

The use of flexible plastic substrates, including PET, polyethylene naphthalate, polyethersulfone and ethylene-tetra-cyclododecene co-polymer, is of great interest in the development of flexible displays. They can contribute to a cost reduction in the production process by allowing the use of the roll-to-roll deposition technique to provide thin, lightweight and flexible optoelectronic devices with a large area [23,31–35]. In this study, the PET substrate film was chemically modified to induce hydrophilic groups on the surface in an attempt to develop a robust layered architecture of Fe(III)-tosylate and EDOT, which was subsequently polymerized to form a smooth and uniform PEDOT coating. Incorporating glycerol as a secondary dopant, the VPP reaction rates were controlled using pyridine in order to determine the optimal kinetic conditions of PEDOT VPP in terms of the surface roughness, conductivity and transparency.

2. Experimental section

2.1. Materials

Fe(III) tosylate, $(Fe(OTs)_3$, 40% solution in *n*-butanol, Baytron C) as an oxidizing agent and dopant were received from Bayer AG. The 3,4-ethylenedioxythiophene (EDOT), all solvents and reagents such as butanol, ethanol, acetone, ethylene diamine (EDA), glycerol, pyridine (referred to here as Py) were purchased from Aldrich and used as supplied. The substrate materials used in this study were plain glass plates and PET films, which were biaxially stretched at 100 μm thickness and supplied by Hwasung Co. Ltd., Korea.

2.2. Surface treatment

The PET film was cleaned twice in acetone prior to use. The film was placed in a glass chamber, which contains EDA to evaporate and fill therein, for the gas-phase EDA treatment of PET films at 40 °C for 10–40 min in the atmospheric pressure. The EDA-treated PET films were rinsed in DI (deionized) water in order to completely remove the EDA, which was checked with litmus paper, and dried at 50 °C for 10 min prior to use.

2.3. Oxidative polymerization of EDOT with Fe(OTs)$_3$ by VPP

The EDA-treated PET was coated with a 20 wt.% oxidant Fe(OTs)$_3$ solution in butanol by spin-coating. Various amount of pyridine and glycerol was added to the Fe(OTs)$_3$ solution. After drying, the samples were transferred to a gas-phase polymerization chamber using a similar experimental setup and method as reported elsewhere [2]. The chamber was flushed with nitrogen during polymerization, and heated to 50 °C. The EDOT was placed at the bottom of the chamber and the vapor-phase polymerization was carried out for 30 min in the atmospheric pressure, and the samples were then heated to 50–90 °C for 30 min. The samples were then washed sequentially with ethanol and DI water. Finally, the PEDOT film was dried to remove the residual solvents at 80 °C for 20 min.
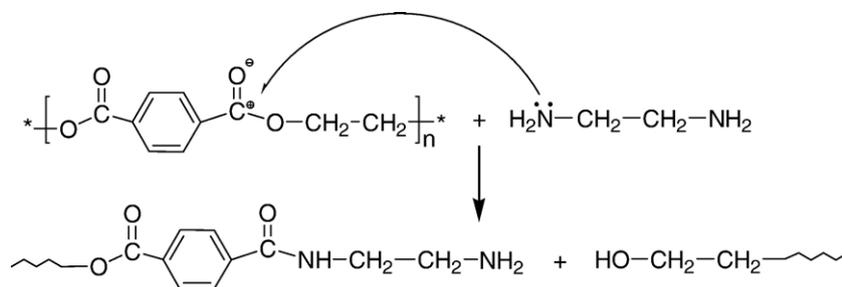
Scheme 1. Vapor-phase reaction of EDA with the ester groups of the PET films.

X-Ray photoelectron spectroscopy (ESCA 2000, VG MICROTECH) equipped with Al Kα radiation source (hν = 1486.6 eV) was used to examine the pristine PET and EDA-treated PET films. Argon ion sputtering was utilized in order to perform depth profiles or to avoid surface contamination of the measurements. The angle between the photon beam and the analyser axis was 90°. The X-ray source was operated at 13 kV, with an emission current of 13 mA. Atomic force microscopy (Auto Probe CP Research, Thermo Microscopes, USA) was performed in contact mode to analyze the film surface morphology at room temperature. The piezoelectric scanner was calibrated using a 1.0 mm grating in the x- and y-directions and in the z-direction using several conventional height standards. The tips were V-shaped silicon (cantilevers). All data manipulations and image processing were carried out using Proscan 1.7 software. All surface roughness values used in this study are the root-mean-square roughness. The conductivity of the samples was measured using a four-point probe (Jandel Engineering Ltd.) connected to a Keithly 2400 source meter. The probe was equipped with four spring-loaded tungsten carbide needles spaced 1 mm apart. The conductivity of the PEDOT film coated on the glass plate was calculated from the surface resistivity and the film thickness, which was measured by FE–SEM (a JEOL JSM-7000F FESEM, voltage of 5.0 kV). The transmittance of the PEDOT films was measured using UV–VIS spectroscopy (spectrophotometer HP 8452). The pH was determined by dipping an electrode of a digital pH meter (Model UB-10 DENVER) into a 0.014 M Fe(TOs)$_3$ solution in butanol. The pH of the initial solution was taken and a 0.15 M solution of pyridine in butanol was then added and subsequent pH obtained. The contact angle was measured using the sessile drop method with a contact angle meter (GBX DIGIDROP-Scientific Instrumentation) equipped with WINDROP++ software version 4.10. Each contact angle was taken as an average measured from three different samples prepared under similar experimental conditions.

3. Results and discussion

3.1. Surface treatment

The purpose of the PET-surface treatment was to create an interfacial interaction between the PET substrate and tosylate as well as PEDOT desirably avoiding organic binders to be used. In this study, vapor-phase EDA was used to induce hydrophilic groups on the PET surface via polymer aminolysis reactions (Scheme 1). In the reaction, EDA is a nucleophile agent and, thus, attacks the carbon in the ester groups to form amide and amine groups on the PET backbone chains.
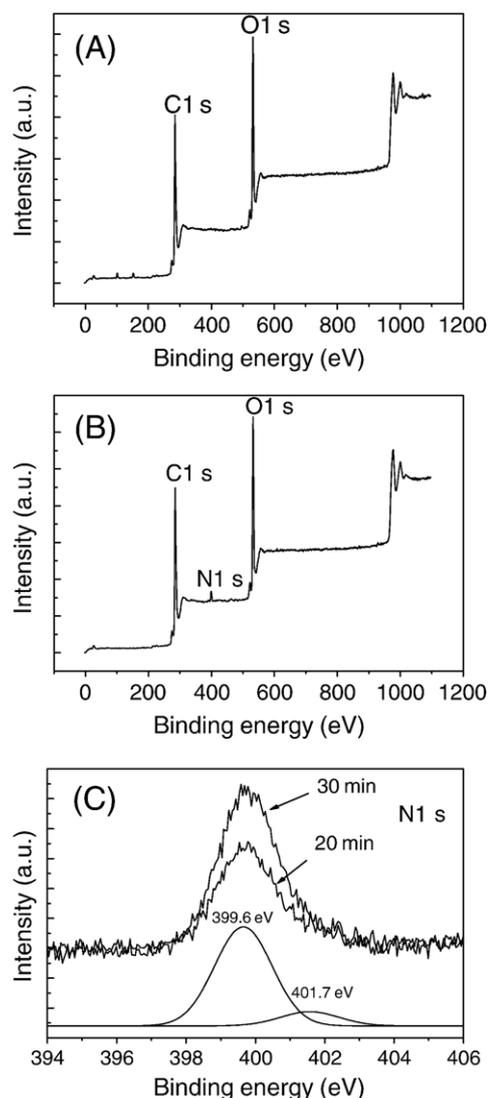
Fig. 1. XPS spectra of the untreated PET films (A), EDA-treated PET films (B), and the high-resolution XPS analysis of N1s peaks of EDA-treated PET films for different treatment times (C). The deconvoluted peaks of the EDA-treated PET for 20 min in (C) show amine and amide N–C bonds at 399.6 and 401.7 eV, respectively. All EDA treatments were performed at 40 °C.
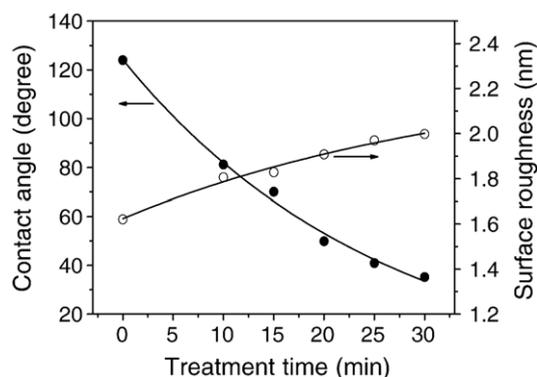
Fig. 2. Water contact angle and surface roughness of EDA-treated PET substrate films measured as a function of the EDA treatment time.

Fig. 1 (A) shows a low-resolution XPS spectrum of an untreated PET film. There are three peaks at 286, 534 and 990 eV, corresponding to the carbon 1s (C1s), oxygen 1s (O1s) and oxygen Auger peaks, respectively [36]. In Fig. 1 (B), the XPS of the EDA- treated PET film also revealed these Auger peaks but with new peak at 399.6 eV corresponding to N1s bonding. High-resolution XPS analysis of this N1s peak of the EDA-treated PET film can be seen in Fig. 1C, which can be deconvoluted as two types of N bonding, 399.6 eV and 401.7 eV. The 399.6 eV peak was assigned to the N–C bond of the amine groups [37–39], whereas the higher binding energy peak at 401.7 eV was assigned to C–N bonding in the amide groups [39,40]. Fig. 1C also shows that the N content increases with an increment of EDA-vapor treatment time. Consequently, it is demonstrated that the aminolysis of PET with EDA results in the formation of amine as well as amide groups on the surface of PET substrate films. These chemical changes can lead to an improvement in hydrophilicity of PET films due to the basic nature of amine groups. Furthermore, it is believed that they can serve as hydrogen bonding sites with EDOT monomers and PEDOT to give an enhanced adhesion to the PET substrates.

Fig. 2 shows the water contact angle and surface roughness of the PET films as a function of the EDA treatment time. The figure shows that the contact angle of the PET substrate decreases gradually with increasing treatment time (up to 30 min) from 124° for the pristine PET film to 35° for the EDA-treated PET film. The large decrease in contact angles can be ascribed to a significant increment of the polar force of the surface free energy due to the formation of amine groups. Meanwhile, the surface roughness of the treated-PET film increases slightly with increasing treatment time from 10 to 30 min but it remains within 2.0 nm. It is believed that the EDA treatment does not deteriorate the surface roughness of PET films substantially.

Fig. 3 shows FE–SEM images of the EDA-treated PET surfaces. No physically-degradative changes can be observed on the EDA-treated PET films at 40 °C between 10 and 30 min. However, significant surface cracking was observed at the treatment time of 40 min in the length scale of few micrometers. Therefore, it was supposed that the optimal treatment time of EDA at 40 °C lies in 20–25 min. Unless stated otherwise, a 20 min EDA treatment was used in the remaining experiments.

3.2. Effect of a weak base

Fig. 4A shows the surface resistivity and surface roughness of the PEDOT coated on EDA-treated PET films as a function of the Py/Fe(OTs)$_3$ molar ratio. The surface resistivity decreases with an increasing Py concentration and shows a minimum of 465 Ω/sq at a Py ratio of ∼0.5. The surface resistivity then increases with the Py concentration. Similarly, the surface roughness decreases with increasing Py concentration and also
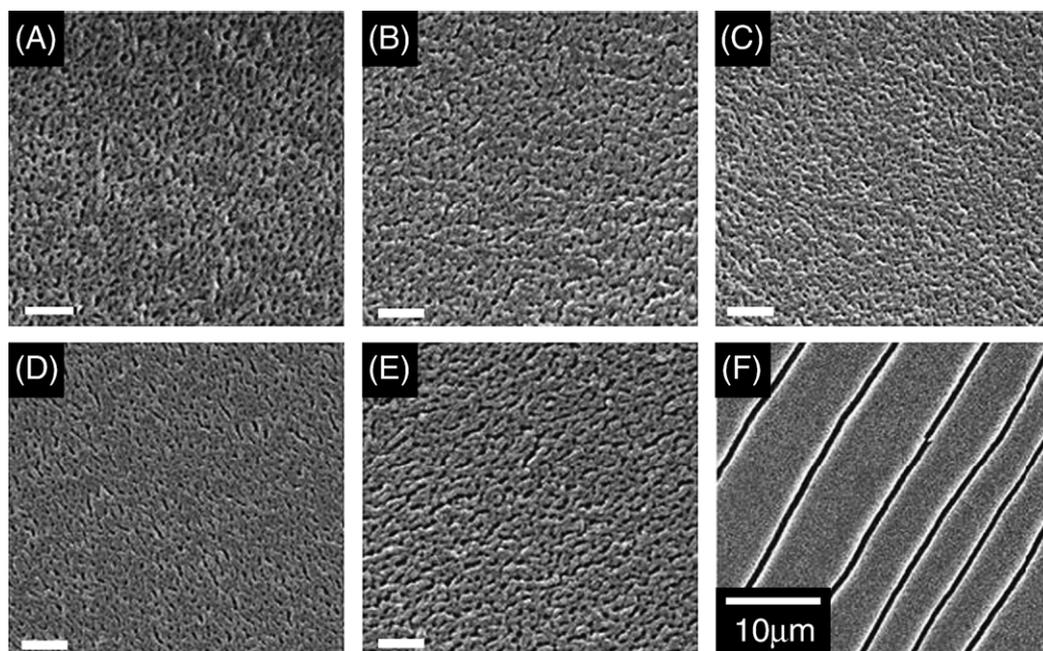

Fig. 3. FE–SEM images of PET film surfaces treated with EDA for (A) 0, (B) 15, (C) 20, (D) 25, (E) 30 and (F) 40 min at 40 °C in the gas phase. The scale bar represents 200 nm for A through E.
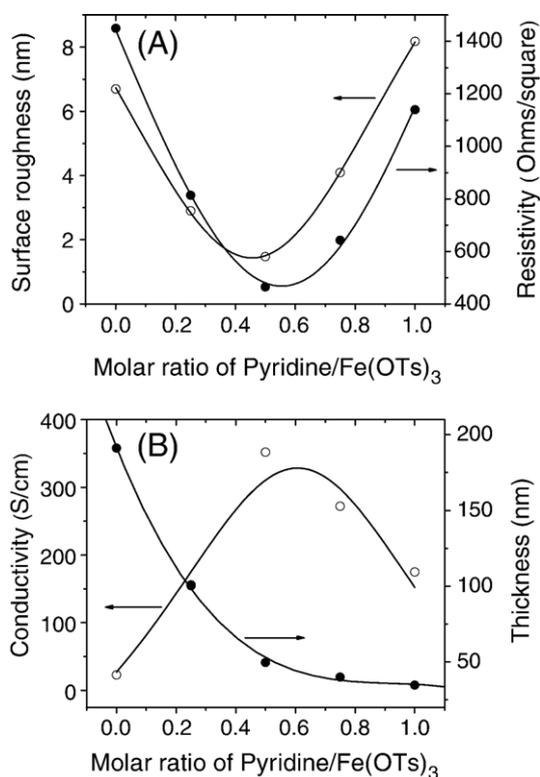
Fig. 4. Surface roughness and the surface resistivity of the PEDOT-coated PET films (A) to be compared with the conductivity and thickness of a PEDOT coating on glass substrates (B) at various molar ratios of pyridine/Fe(OTs)$_3$.

Fig. 5. AFM height profiles of PEDOT films at different Py/Fe(OTs)$_3$ ratios: (A) 0, (B) 0.25, (C) 0.5, (D) 0.75, (E) 1.0.

because the thickness of the PEDOT layer decreases with increasing Py concentration (Fig. 4B). The transparency of Py-incorporated PEDOT coating is considered to be associated with the basic nature of Py, which can influence the molecular weight and doping level of PEDOT during the vapor-phase polymerization.

A basic inhibitor such as amine increases the pH of the reaction media, and subsequently decreases the redox activity of Fe(OTs)$_3$. According to Scheme 2, the electronic semi-equilibrium relation may be described as

$$Fe^{3+}(OTs)_3 + e^- + H^+ \rightarrow Fe^{2+}(OTs)_2 + OTs^- H^+ \tag{1}$$
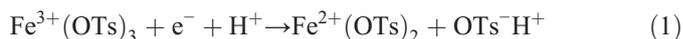
Subsequently, the electrode potential of the Fe$^{(3+)}$/Fe$^{(2+)}$ redox couples can be expressed as a function of pH using the Nernst equation:

$$
\begin{aligned}
E &= E^0 + \left(\frac{2.3RT}{nF}\right) \log \frac{[Fe^{3+}][H^+]}{[Fe^{2+}]} \\
&= E^0 + \left(\frac{2.3RT}{nF}\right) \log \frac{[Fe^{3+}]}{[Fe^{2+}]} + \left(\frac{2.3RT}{nF}\right) \log[H^+] \\
&= E^* + \left(\frac{2.3RT}{nF}\right) \log[H^+] \tag{2}
\end{aligned}
$$

where E is the electrode potential of the Fe$^{(III)}$/Fe$^{(II)}$ redox couple in the Fe(OTs)$_3$–Py solution, E^o is the potential of the

reaches a minimum of 1.47 nm at a similar Py ratio of ∼ 0.5. The same experiments were carried out using a glass substrate instead of PET to confirm these results because it is generally difficult to measure the PEDOT coating thickness on the PET substrate with accuracy. The PEDOT thickness on the galss substrate was measured by FE–SEM and the conductivity was calculated from the surface resistivity and the thickness (Fig. 4B). As can be seen, the conductivity reaches a maximum of 350 S/cm at a Py ratio of 0.5, which is approximately 16 times higher than that of the PEDOT without Py (22 S/cm).

Fig. 5 shows the AFM surface profiles of the PEDOT produced at different Py/Fe(OTs)$_3$ ratios. Fig. 5 (A) shows the surface profiles of PEDOT without Py, which does not show a smooth morphology. A distinct improvement of the surface roughness is observed at higher Py concentrations up to 0.5 (Fig. 5B and C). At Py concentrations >0.75, larger grains are likely formed and the surface roughness obviously increases (Fig. 5D and E). Conclusively, the surface roughness is influenced considerably by the Py concentration, and a minimum roughness of 1.47 nm (Fig. 4A) can be obtained at a Py ratio of 0.5. This suggests that Py has a substantial effect on the conductivity and surface roughness in the VPP of PEDOT.

The effect of Py on the transparency of PEDOT was investigated using UV–VIS spectroscopy in Fig. 6. It is clear that Py also plays an important role in the transparency of PEDOT coating. Transmittance increases with increasing Py concentration over wavelengths ranging from 320 nm to 750 nm. In particular, the transmittance could exceed 90% at a Py concentration >0.75
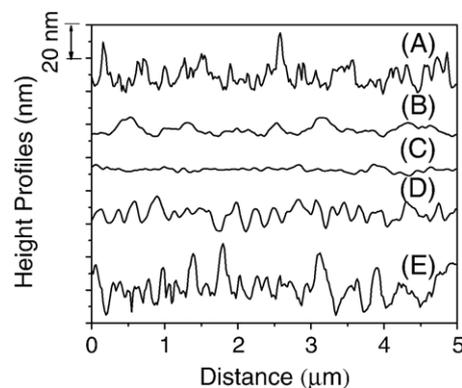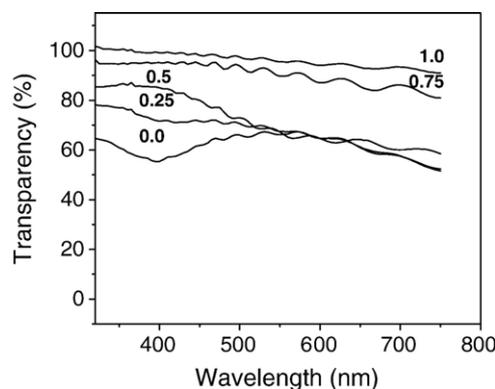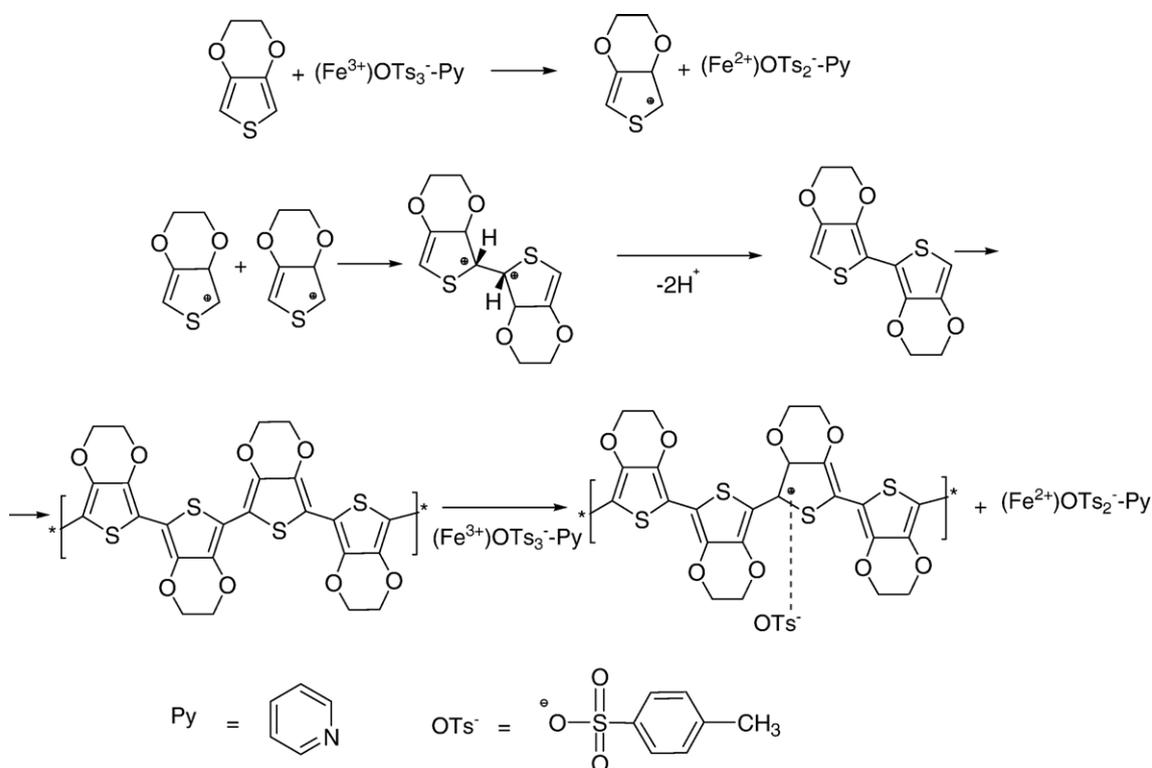

Fig. 6. Transparency of PEDOT films as a function of the pyridine/Fe(OTs)$_3$ molar ratio.

Scheme 2. Oxidative polymerization of EDOT in the presence of Py.

reference electrode, (2.3 RT/nF) is the Nernst factor, and log [H$^+$] is the pH of the Fe(OTs)$_3$ solution. The Nernst factor, 2.3 RT/nF, includes the Gas Law constant (R), Faraday's constant (F), the temperature in degrees Kelvin (T) and the charge of the ion (n). E* is the standard redox potential when [Fe$^{(3+)}$]=[Fe$^{(2+)}$] and [H$^+$]=1 M. Accordingly, the electrode behavior is solely dependent on pH because the Fe(OTs)$_3$ concentration, R, T and F are constants. Fig. 7 shows that the pH of the Fe(OTs)$_3$ solution increases with increasing Py concentration, which subsequently gives reduced electrode potentials. This suggests that the reduction of Fe$^{(3+)}$ to Fe$^{(2+)}$ becomes more difficult with an increased Py concentration and, thus, results in a decrease in the PEDOT layer thickness (Fig. 4B). In addition, Py coordinates with the Fe(OTs)$_3$ through the successive substitution of Py with the alcohol ligands via the unbonded electrons in N. It is considered that this can decrease the polymerization reaction rates.

Scheme 2 gives a schematic of the oxidative polymerization of EDOT, which is a similar polymerization mechanism in the presence of imidazole as a weak base [30]. Fe(OTs)$_3$ oxidizes EDOT, and the cationic EDOT radical dimerizes and is rapidly stabilized via the base-assisted removal of two protons, whereas Fe$^{(3+)}$ is reduced to Fe$^{(2+)}$. Additional Fe(OTs)$_3$ oxidizes the dimers, and the chain growth proceeds as a classical step-polymerization. Fe(OTs)$_3$ also oxidizes the growing chains, leaving the PEDOT in the doped (conducting) state [30] Therefore, the yield and quality of the product obtained by the oxidative polymerization depend on the reactivity of the oxidants. Very rapid polymerization kinetics causes the prepolymerized nanoscopic droplets to precipitate onto the substrate, which

increases the surface roughness [30]. PEDOT films produced at a high redox reactivity often provides defect sites and a low degree of intermolecular order, ultimately limiting their use in electronic devices. For this reason, it is believed that high quality PEDOT can be obtained by controlling the polymerization rates to minimize the side reactions and the number of defects.

As discussed earlier, a Py/Fe(OTs)$_3$ ratio of 0.5 was found to be the optimum in terms of the conductivity and surface roughness. This suggests that the oxidative reactivity of the Fe(OTs)$_3$-pyridine solution with a Py concentration of 0.5 is appropriate for the VPP of EDOT. The optimized polymerization rate can promote the production of a higher molecular weight PEDOT and enhances the stability of the radical cations by delocalization over a planar conjugated oligomer or polymer. Py also acts as a reducing agent as a result of its unbonding
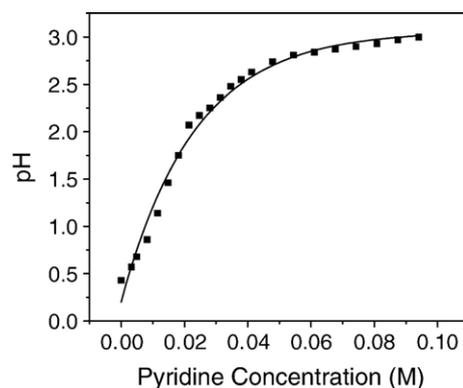
Fig. 7. pH of Fe(OTs)$_3$ solution as a function of the Py concentration.

electron transfer to the cation radical in the conducting polymer, which prevents PEDOT from being overdoped to give an enhanced transparency [30] (see also Fig. 6). However, when the Py concentration is higher than 0.5, it is believed that pyridine acts as an impurity, which may well accumulate in PEDOT and disturb the electric charge current. Therefore, it can be concluded that a $Py/Fe(OTs)_3$ molar ratio of 0.5: 1 is the optimal PEDOT polymerization condition in a butanol solvent.

3.3. Effect of glycerol

A glycerol-doped PEDOT (referred to here as G-PEDOT) was prepared at a fixed $Fe(OTs)_3$ concentration of 20 wt.% and a $Py/Fe(OTs)_3$ of 0.5:1 molar ratio in butanol. Fig. 8A shows the surface resistivity and surface roughness of the PEDOT coating on the PET substrate film as a function of glycerol concentration in the unit of weight% with respect to the $Py/Fe(OTs)_3$ butanol solution. It can be seen that the surface resistivity decreases with increasing glycerol concentration, reaching a minimum value of 289 Ω/sq at a glycerol concentration of 5 wt.%. The surface roughness is maintained at ca. 2 nm with up to 5 wt.% glycerol, which increases rapidly at higher concentrations of glycerol. The same experiment was also carried out for a glass substrate instead of the PET substrate in order to estimate the conductivity of the glycerol-doped PEDOT coating using accurate values of the surface resistivity and film thickness (Fig. 8B). As with the surface resistivity measured for the PET substrate in Fig. 8A, the

Fig. 9. Transparency of PEDOT films for various glycerol concentrations at a fixed molar ratio of pyridine/Fe(OTs)$_3$ at 0.5.

conductivity reaches a maximum value of 500 S/cm at a glycerol concentration of ca. 5 wt.%. Therefore, considering both conductivity and surface roughness, 4–5 wt.% of glycerol appears to be the optimal doping concentration of glycerol.

An increase in conductivity in the presence of glycerol has been reported for PEDOT–PSS systems as a secondary dopant [24–26]. In addition, the device configuration using G–PEDOT is considered to facilitate the hole transport and, thus, can lead to an improved balance in the electron and hole currents. However, it should be noted that glycerol is an electrical insulator by nature, which may well lower the film conductivity at excessive concentrations. It can also interfere sterically with the reaction between EDOT and Fe^{3+} to form large PEDOT granules and rougher surface characteristics. For these reasons, we believe that the glycerol concentration >5 wt.% can be regarded as being excessive in the VPP of PEDOT and resultantly deteriorates the surface smoothness as well as the conductivity of PEDOT coating.

Fig. 9 shows that the G-PEDOT coating at a glycerol concentration of 5 wt.% has higher transparency than the PEDOT coating (0 wt.% of glycerol) although its thickness is higher. It is supposed that the incorporation of glycerol, which has a lower absorbtivity than PEDOT, gives an enhanced transparency of the glycerol/PEDOT composite film unless the amount of glycerol is excessive to form a PEDOT granule or
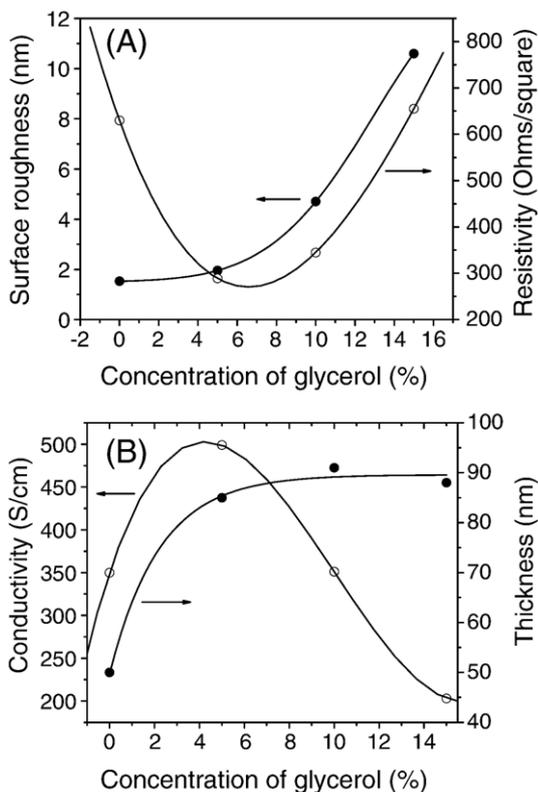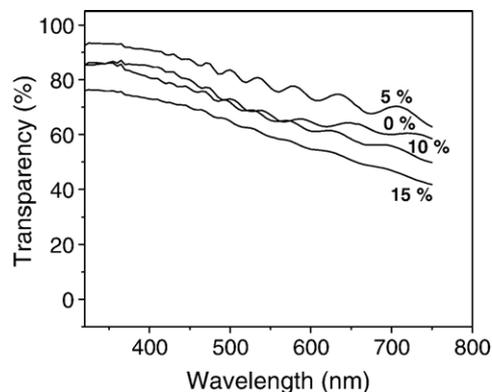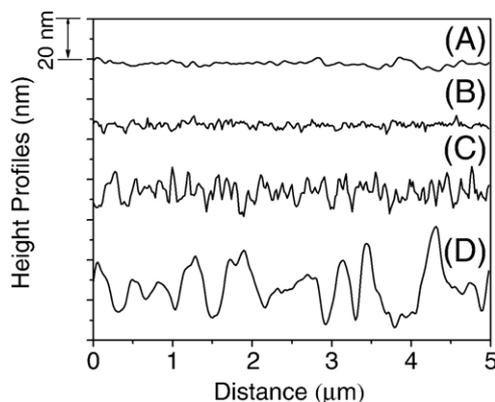

Fig. 8. Surface roughness and the surface resistivity of PEDOT-coated PET films (A), and the conductivity and thickness of PEDOT coating on glass substrates (B) as a function of glycerol concentrations at a fixed molar ratio of pyridine/Fe (OTs)$_3$ at 0.5.

Fig. 10. AFM height profiles of PEDOT films at a fixed molar ratio of pyridine/Fe(OTs)$_3$ at 0.5 for various glycerol concentrations: (A) 0, (B) 5, (C) 10, (D) 15 wt.%.

rough surface. As confirmed with the glycerol concentration >10 wt.%, transparency of the G-PEDOT coating decreases with the glycerol concentration mainly due to the increased surface roughness, PEDOT gradules, and PEDOT-coating thickness. (Fig. 10).

4. Conclusions

PEDOT was deposited on PET substrate films using a vapor-phase polymerization technique. The surface of the PET substrate films was treated by the aminolysis reactions to create amine and amide groups for the hydrophilic interaction with the $Fe(OTs)_3$ butanol solution and for the hydrogen bonding with EDOT and PEDOT. Pyridine and glycerol influenced the conductivity, transparency and surface roughness of the PEDOT coating to a large extent. The PEDOT coating exhibited an optimal condition of Py and glycerol concentrations at 5.0 molar ratio and 4–5 wt.%, respectively, giving a thickness ranging from 50 to 100 nm, a conductivity of ~500 S/cm, a transparency >70%, and a surface roughness <2 nm.

Acknowledgements

References

[1] F. Jonas, L. Schrader, Synth. Met. 41 (1991) 831.
[2] B. Winther-Jensen, J. Chen, K. West, G. Wallace, Macromolecules 37 (2004) 5930.
[3] B. Winther-Jensen, K. West, Macromolecules 37 (2004) 4538.
[4] D.M. Welsh, A. Kumar, E.W. Meijer, J.R. Reynolds, Adv. Mater. 11 (1999) 1379.
[5] L.S. Romana, A.C. Arias, M. Theander, M.R. Andersson, O. Inganas, Braz. J. Phys. 33 (2003) 367.
[6] M.Y. Song, K.J. Kim, D.Y. Kim, Sol. Energy Mater. Sol. Cells 85 (2005) 31.
[7] D. Wakizaka, T. Fushimi, H. Ohkita, S. Ito, Polymers 45 (2004) 8561.
[8] W.H. Kim, A.J. Makinen, N. Nikolov, R. Shashidhar, H. Kim, Z.H. Kafafi, Appl. Phys. Lett. 80 (2002) 3844.
[9] C.W. Tang, S.A. Vanstlyke, Appl. Phys. Lett. 51 (1987) 913.
[10] W.Y. Chou, S.T. Lin, H.L. Cheng, M.H. Chang, H.R. Guo, T.C. Wen, Y.-S. Mai, J.B. Horng, C.W. Kuo, F.C. Tang, C.C. Liao, C.L. Chiu, Thin Solid Films 515 (2007) 3718.
[11] T.V. Voudenbergh, J. Wildeman, P.W.M. Blom, J.J.A.M. Bastiaansen, B.M.W.L. Wos, Adv. Funct. Mater. 14 (2004) 677.
[12] Z. Kafafi, Organic Electroluminescence, Taylor & Francis, Boca Raton, 2005.
[13] J. Shinar, Organic Light-Emitting Devices, Springer-Verlag, New York, 2004.
[14] T.A. Skotheim, R.L. Elsenbaumer, J.R. Reynolds, Handbook of Conducting Polymer, Second EditionMarcel Dekker, New York, 1998.
[15] B.L. Groenendaal, F. Jonas, D. Freitag, H. Pielartzik, J.R. Reynolds, Adv. Mater. 12 (2000) 481.
[16] F. Jonas, G. Heywang, Electrochim. Ecta 39 (1994) 1345.
[17] M. Kemerink, S. Timpanaro, M.M. De Kok, E.A. Meulenkamp, F.J. Touwslager, J. Phys. Chem. B 108 (2004) 18820.
[18] A.M. Higgins, S.J. Martin, P.C. Jukes, M. Geoghegan, R.A.L. Jones, S. Langridge, R. Cubitt, S. Kirchmeyer, A. Wehrume, I. Grizzie, J. Mater. Chem. 13 (2003) 2814.
[19] P.C. Jukes, S.J. Martin, A.M. Higgins, M. Geoghegan, R.A.L. Jones, S. Langridge, A. Wehrum, S. Kirchmeyer, Adv. Mater. 6 (2004) 807.
[20] M.P. De Jong, L.J. Van Ijzendoorn, M.J.A. De Voigt, Appl. Phys. Lett. 77 (2000) 2255.
[21] L. Groenendaal, G. Zotti, F. Jonas, Synth. Met. 118 (2001) 105.
[22] J. Kim, E. Kim, Y. Won, H. Lee, K. Suh, Synth. Met. 139 (2003) 485.
[23] B. Winther-Jensen, F.C. Krebs, Sol. Energy Mater. Sol. Cells 90 (2006) 123.
[24] A.J. Ma kinen, I.G. Hill, R. Shashidhar, N. Nikolov, Z.H. Kafafi, Appl. Phys. Lett. 79 (2001) 557.
[25] T. Granlund, L.A.A. Pettersson, O. Inganas, J. Appl. Phys. 89 (2001) 5897.
[26] J. Huang, P.F. Miller, J.S. Wilson, A.J. De Mello, J.C. De Mello, D.D.C. Bradley, Adv. Mater. 15 (2005) 290.
[27] J.Y. Kim, J.H. Jung, D.E. Lee, J. Joo, Synth. Met. 126 (2002) 311.
[28] R. Kiebooms, A. Aleshin, K. Hutchison, F. Wudl, A. Heeger, Synth. Met. 101 (1999) 436.
[29] D.M. De Leeuw, P.A. Kraakman, P.F.G. Bongaerts, C.M.J. Mutsaers, D.B.M. Klaassen, Synth. Met. 66 (1994) 263.
[30] Y.H. Ha, N. Nikolov, S.K. Pollack, J. Mastrangelo, B.D. Martin, Adv. Funct. Mater. 14 (2004) 615.
[31] M. Izu, T. Ellison, Sol. Energy Mater. Sol. Cells 78 (2003) 613.
[32] T. Makela, S. Jussila, H. Kossonen, T.G. Backlund, H.G.O. Sandberg, H. Stubb, Synth. Met. 153 (2005) 285.
[33] S.C. Lima, S.H. Kim, J.H. Lee, H.Y. Yu, Y.S. Park, D.J. Kim, T.Y. Zyunga, Mater. Sci. Eng. B 121 (2005) 211.
[34] M.J. Lee, C.P. Judge, S.W. Wright, Solid State Electron. 44 (2000) 1431.
[35] A.Y. Natori, C.D. Canestraro, L.S. Romanb, A.M. Ceschin, Mater. Sci. Eng. B 122 (2005) 231.
[36] G. Beamson, D. Briggs, High Resolution XPS of Organic Polymers: The Scienta ESCA300 Database, Wiley, Chichester, England, 1992.
[37] A. Snis, S.F. Matar, O. Plashkevych, H. Agren, J. Chem. Phys. 111 (1999) 9678.
[38] P. Snauwaert, R. Lazzaroni, J. Riga, J.J. Verbist, D. Gonbeau, J. Chem. Phys. 92 (1990) 2187.
[39] G.A. Schick, Z. Sun, Langmuir 10 (1994) 3105.
[40] J.F. Moulder, W.F. Stickle, P.E. Sobol, K.D. Bomben, in: J. Chastain (Ed.), Handbook of X-Ray Photoelectron Spectroscopy, Perkin–Elmer, Minneapolis, 1992.